

# INTERNATIONAL SOCIETY FOR SOIL MECHANICS AND GEOTECHNICAL ENGINEERING



*This paper was downloaded from the Online Library of the International Society for Soil Mechanics and Geotechnical Engineering (ISSMGE). The library is available here:*

<https://www.issmge.org/publications/online-library>

*This is an open-access database that archives thousands of papers published under the Auspices of the ISSMGE and maintained by the Innovation and Development Committee of ISSMGE.*

*The paper was published in the proceedings of the 7<sup>th</sup> International Conference on Earthquake Geotechnical Engineering and was edited by Francesco Silvestri, Nicola Moraci and Susanna Antonielli. The conference was held in Rome, Italy, 17 - 20 June 2019.*

## Site response analysis to evaluate vertical-to-horizontal spectrum ratio

C.C. Tsai & P.C. Liu

*National Chung Hsing University, Taichung, Taiwan*

**ABSTRACT:** A vertical-to-horizontal (V/H) response spectral ratio of 2/3 (Newmark and Hall, 1978) is commonly adopted in earthquake engineering practice for assessing the magnitude of vertical motion. However, recent observations from earthquake records indicate that this ratio can be exceeded considerably in some circumstances. In this study, the factors that could influence the V/H ratio are evaluated on the basis of the vertical and horizontal site response analyses. Different intensities of vertical and horizontal motions fixed with a constant V/H ratio are propagated through generic sites with various groundwater tables, soil porosities, and wave velocity profiles. The V/H ratio on the ground surface is then calculated and compared with that at the bedrock. Results show that the V/H ratio increases with the intensity of input motion. In addition, a site with a shallow groundwater table and low porosity tends to amplify the V/H ratio.

### 1 INTRODUCTION

Vertical ground motions are often considered in the seismic design of critical structures, such as nuclear power plants and dams, but not for standard structures. Therefore, prediction for the vertical component of ground motions has received considerably less attention than those for the horizontal component. However, recent studies suggest that the effect of the vertical ground-motion component can also be remarkable for the seismic response of ordinary highway bridges on sites located within approximately 15 km of major faults (Kunnath et al., 2008; Gülerce and Abrahamson, 2010). Therefore, an engineering need exists to predict vertical ground motions.

Although the magnitude of vertical ground motion is generally smaller than its horizontal counterpart (Yang and Yan, 2009), very strong vertical ground motions have been recorded in recent seismic events, including the 1994 Northridge earthquake (the ratio of vertical to horizontal peak acceleration, i.e.,  $V/H > 1.5$ ; NCEER, 1997), the 1995 Kobe earthquake ( $V/H = 2$ ; Yang and Sato, 2000), and the 1999 Chi-Chi earthquake and 2007 Wenchuan earthquake ( $V/H > 1$  in some areas near the epicenter; Wang, 2008).

Previous work on the characterization of vertical motions has focused on vertical-to-horizontal ratios (V/H ratios) (e.g., Ambraseys and Douglas, 2003). The V/H ratios are typically used to modify a horizontal response spectrum (uniform hazard spectrum or scenario spectrum) to produce a corresponding vertical spectrum. Therefore, the common procedure for generating vertical design spectra, as documented in many seismic provisions and codes, is to simply multiply a factor (typically a value of 2/3) to the horizontal design spectra, wherein the response spectral ratio between the vertical and horizontal motions is assumed to be a constant less than 1 over the entire period of interest and for all site conditions. However, recent observations from earthquake records suggest that the commonly adopted V/H response ratio of 2/3 (Newmark and Hall, 1978) may be exceeded considerably at short periods in the near-source distance range (Bozorgina et al., 1995).

The principal limitation of using constant V/H ratios is that the vertical component may scale differently from the horizontal with respect to the moment magnitude (M), source-site distance, and site condition (Gülerce and Abrahamson, 2011; Stewart et al., 2016).

Nonlinearity strongly influences the horizontal component at high frequencies for soft sites while exerting a relatively small effect on the vertical component, which may cause V/H ratios to rise in such conditions (Yang and Lee, 2007). In this study, the factors that could influence the V/H ratio are evaluated on the basis of the vertical and horizontal site response analyses.

## 2 WAVE PROPAGATION OF VERTICAL MOTION

Generally, the vertical motions are the consequence of compressional stresses that are mainly transmitted by pore fluids. Liu and Tsai (2018) analyzed three component records of five downhole arrays and considered different geological conditions, ground water tables, and intensity of motions to evaluate the differences of wave propagation in the vertical and horizontal directions. The location of ground water table influences the amplification of vertical motion (e.g., amplitude and nonlinearity) but does not affect the amplification of horizontal motion. Given these observations, Tsai and Liu (2017) developed a benchmark approach for equivalent linear vertical site response analyses with a focus on the modeling of soil nonlinearity. The modeled soil exhibits different nonlinear behaviors in the vertical direction depending on the saturation condition (i.e., above or below the groundwater table). Moreover, the vertical nonlinearity is different from that observed in the horizontal direction. The vertical ground responses predicted by the proposed approach has been validated with downhole measurements associated with different geological conditions, groundwater tables, and shaking intensities.

In this study, the benchmark approach for vertical site response analyses by Tsai and Liu (2017) is adopted for propagating vertical motion. In their procedure, vertical site response analyses can be performed using conventional computer programs by replacing Vs with Vp and replacing the horizontal input acceleration time series with a vertical acceleration time series. However, the critical issue remains on how to handle the soil nonlinearity (i.e., modulus reduction curve and damping curve) in the vertical direction. More details regarding these issues are described later. DEEPSOIL software (Hashash et al., 2016) are used to perform the frequency domain equivalent linear site response.

## 3 ANALYSIS CASES

### 3.1 Soil profile

The hypothetical soil site based on Yang and Yan (2009) is shown in Figure 1a. The soil profile is 30 m deep comprising a surface of clayey sand layer of 10 m and underlying sand layer of 20 m. The mass density of the clayey sand is assumed to be 1800 kg/m<sup>3</sup>, and the density of the sand is 2000 kg/m<sup>3</sup>. The shear wave velocity, Vs, varies from 170 m/s in the clayey sand layer to 350 m/s in the sand layer. The location of the bedrock is assumed to be at the depth of 30 m with a shear wave velocity of 470 m/s. Using the NEHRP site classification system, the site can be categorized as a Site Class D (stiff-soil site).

However, the compressional wave velocity, Vp, is dependent on the ground water table and porosity of soil and rock. The ground water table is assumed at the surface, 5 m, 10 m below the ground surface, and at the bottom of the profile (i.e., dry condition). The Vp below the ground water table assumes a different porosity and is calculated as follows per Biot (1956):

$$V_p^* = \sqrt{\frac{M_{\max}^*}{\rho^*}} = \sqrt{\frac{M_{\max} + \frac{K_f}{n}}{\rho}}, \quad (1)$$

where  $M_{\max}$  is the constrained modulus at the small strain condition that can be obtained by the Vp of dry condition in Figure 1a, n is the porosity of the soil,  $K_f$  is the bulk modulus of fluid (i.e., water), and \* indicates a saturation condition. Three porosities of the soil are

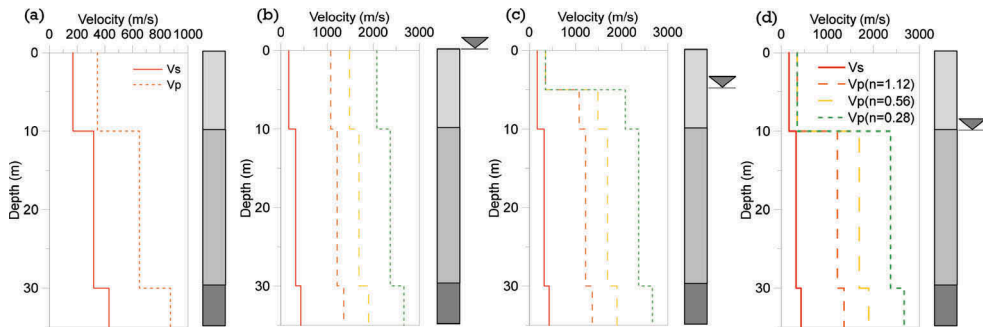


Figure 1. Velocity profile. (a) Dry condition, (b) Ground water table at the ground surface, (c) Ground water table at 5 m below the ground surface, (d) Ground water table at 10 m below the ground surface.

assumed, namely, 1.12, 0.56, and 0.28. The corresponding  $V_p$  profile for the different water table and porosities are shown in Figure 1b, c, and d. The soil column is discretized in the time domain analysis to make sure that maximum passing frequency is 25hz.

### 3.2 Nonlinear curve

The nonlinear behavior of the entire sandy soil is assumed to follow the curves developed by Seed and Idriss (1970), as shown in Figure 2(a). The curves are only applicable for propagating horizontal motions. For the vertical motion analysis,  $M/M_{\max}$  under dry and wet conditions can be constructed based on the  $G/G_{\max}$  curve and Eq. (1). Following the procedure proposed by Tsai and Liu (2017), the  $M/M_{\max}$  is derived and shown in Figure 2. Once the reduction curve of the constrained modulus is determined, the hysteretic damping in the vertical direction can be estimated with hyperbolic model (Hardin and Drnevich, 1972) and Masing rule (Masing, 1926), which are similar to that in the horizontal direction, as shown in Figure 2.

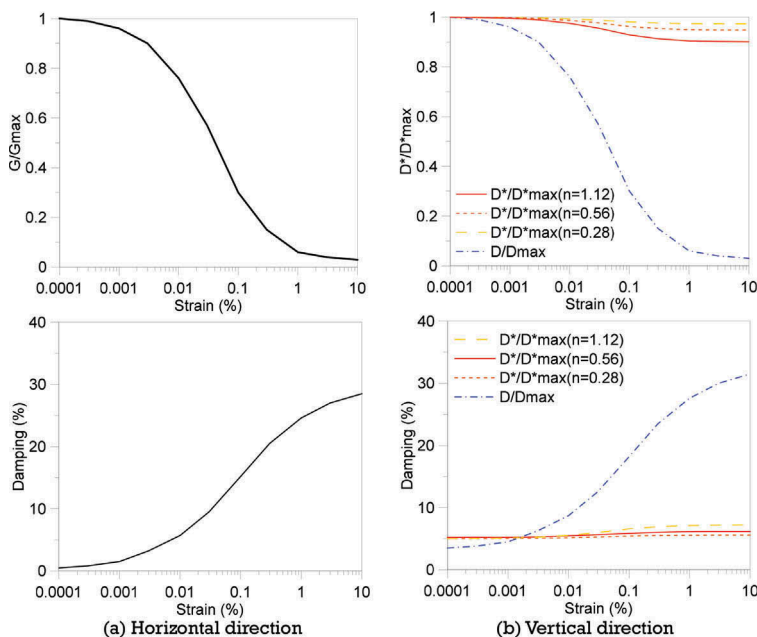


Figure 2. Modulus reduction and damping curve. (a) horizontal direction, (b) vertical direction.

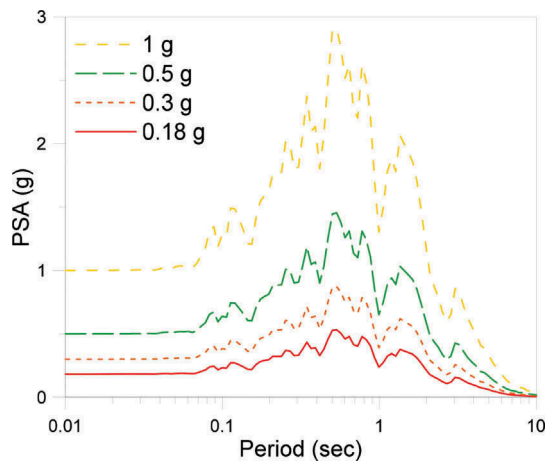


Figure 3. Input bedrock motion.

The  $M/M_{\max}$  is essentially the same as the  $G/G_{\max}$  curve for the dry condition (above ground water table). However, the  $M^*/M^*_{\max}$  of the saturation condition exhibits less nonlinearity due to the high buck modulus of the water. Moreover, different porosities also result in different nonlinearities. As porosity increases, less nonlinearity is exhibited. Therefore, the damping curves of the wet condition do not increase with the strain considerably. However, an additional small strain damping (3%) is added in the vertical direction to account for the energy dissipation due to the interaction of fluid and soil particles (Tsai and Liu, 2017).

### 3.3 Input motion

The input motions used in this study are shown in Figure 3 in terms of acceleration time histories and response spectra at 5% damping. The input motions are obtained at the TCU045 station during the 1999 Chi-Chi earthquake in Taiwan. The peak horizontal acceleration appearing at 17.8 s is 0.18 g. The vertical motions are directly scaled by 2/3. To evaluate the effect of the intensity of input on the V/H ratio, the horizontal motion is scaled to 0.3 and 0.5 g. The vertical motion is fixed with the same V/H ratio of 2/3.

## 4 ANALYSIS RESULTS

### 4.1 Horizontal and vertical responses

Figure 4(a) shows the surface response spectrum of the horizontal and vertical motions under the dry condition (Figure 1a). The bedrock response spectrum is also presented for comparison. The horizontal and vertical motions are amplified, but the amplification of the horizontal motion is more significant than that of the vertical. The horizontal and vertical motions are amplified mostly at 0.6 and 0.2 s corresponding to the site period in the horizontal and vertical directions, respectively. The V/H ratio, as shown in Figure 4 (b), is obtained by directly taking the ratio between the vertical and horizontal spectra. The original ratio (i.e., 2/3 at bedrock) is altered due to the local site effect. The ratio becomes greater than 2/3 at the periods from 0.1 s to 1 s. The shape of the V/H ratio spectrum is similar to the vertical spectrum, wherein both peak values occur at 0.2 s.

Figure 5 shows the strain profiles for the different directions. The strain in the vertical and horizontal directions indicates compression and shear strain, respectively. The obtained compression strain is smaller than the shear strain due to a higher  $V_p$  than  $V_s$ . The results also

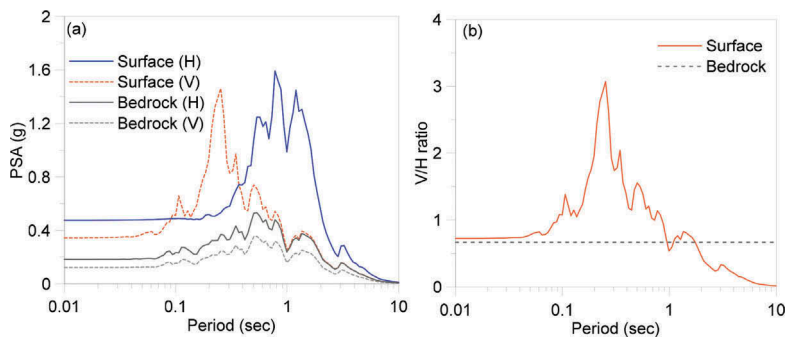


Figure 4. (a) Surface response spectra of the horizontal and vertical motions, (b) V/H ratio under dry condition.

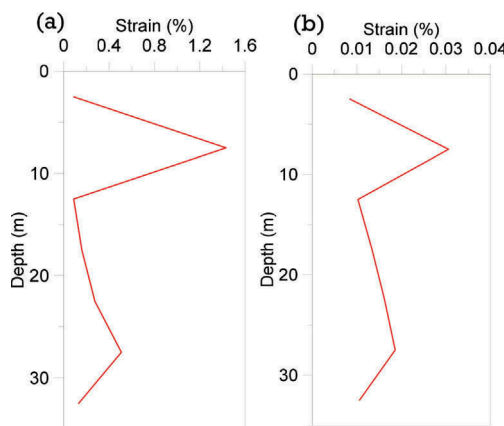


Figure 5. Maximum strain profiles. (a) Horizontal component, (b) Vertical component.

indicate that soil behaves relatively linearly when propagating vertical motions compared with the horizontal motion.

#### 4.2 Influence of ground water table on V/H ratio

Figure 6 shows the V/H ratio for different ground water tables and porosities of the soil. The V/H ratios for the dry and wet conditions are completely different. The dry condition (Figure 6 (a)) shows the dominant periods ( $T_p$ ) of 0.2 s while the  $T_p$  locates at the short period (approximately 0.1 s) at the wet condition (Figure 6 (b)(c)(d)). As the ground water table is lower, the  $T_p$  shifts to a longer period and eventually approaches to 0.2 s, as observed in the dry condition, because the average  $V_p$  becomes lower as the groundwater is lower. However, the change is not remarkable due to a much higher  $V_p$  beneath the groundwater table compared with that above the groundwater table. In addition to the different  $T_p$  of the V/H ratio, the peak values are also different. As the groundwater table becomes low, the V/H ratio increases especially at the  $T_p$ .

Figure 7 shows the compression strain profiles for different groundwater tables. The strain profile is more uniform in the completely dry or completely wet condition. By contrast, the obtained compression strain is very small below the groundwater table but becomes relatively large above the groundwater table because of the sudden change in  $V_p$  above and below the groundwater table (Figure 1). However, the largest compression strain in the vertical direction

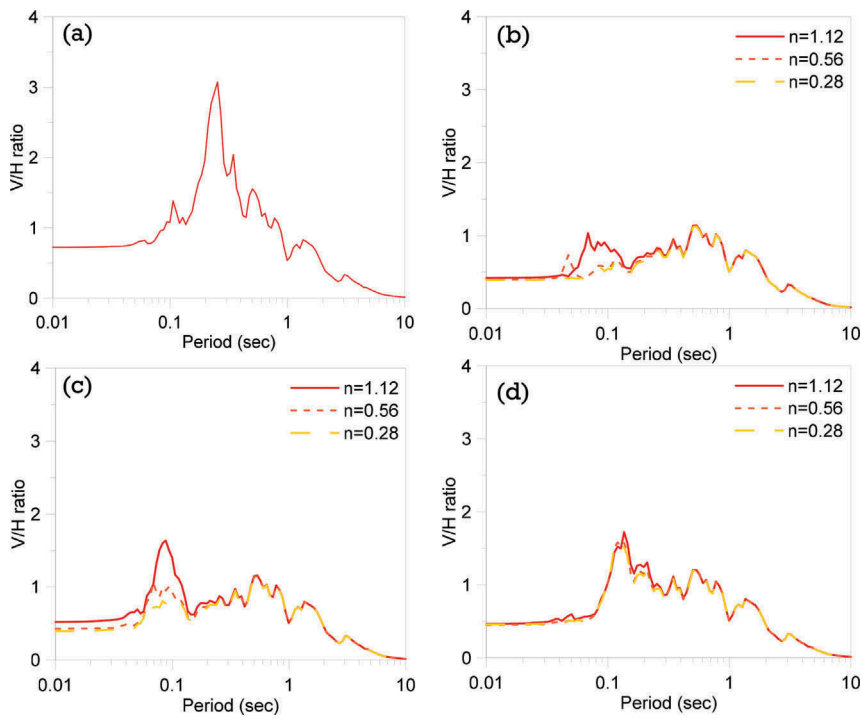


Figure 6. Influence of the groundwater table and void ratio in (a) dry condition, (b) groundwater table at the ground surface, (c) ground water table at 5 m below the ground surface, (d) ground water table at 10 m below the ground surface.

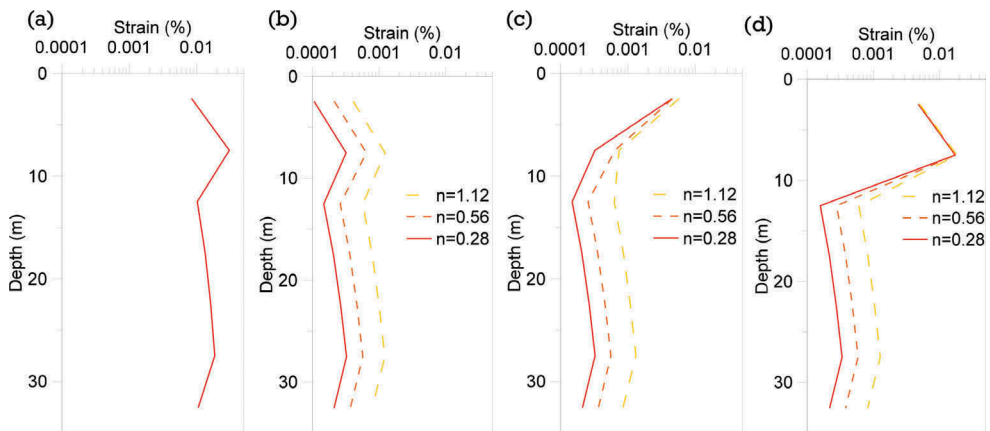


Figure 7. Maximum compression strain profiles. (a) Dry condition, (b) groundwater table at the ground surface, (c) groundwater table at 5 m below the ground surface, (d) groundwater table at 10 m below the ground surface.

is still less than the shear strain in the horizontal direction (Figure 5) due to the high stiffness in the vertical direction. The low compression strain also indicates that the soil behaves linearly when propagating vertical motions especially beneath the groundwater table.

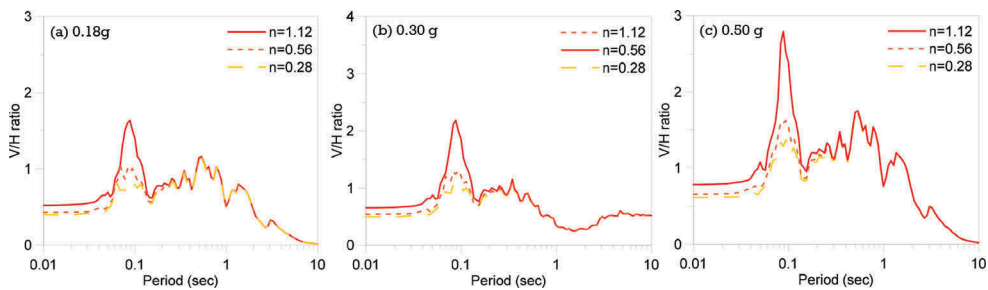


Figure 8. Influence of the intensity of input motion.

#### 4.3 Influence of void ratio

Vertical response is dependent on the soil porosities, which influence the  $V_p$  profile and the nonlinear behavior below the groundwater table. Consequently, it also changes the V/H ratios. As shown in Figure 6, when  $n$  is larger, the peak V/H ratio becomes larger regardless the level of the groundwater table. The influence of  $n$  is significant for the case of water table at the surface and 5 m below the ground surface because the ground surface response is dominated by the  $V_p^*$  that is dependent of  $n$  when the groundwater table is shallow. By contrast, the ground surface response is dominated by the  $V_p$  that is independent of  $n$  when the groundwater table is deep (i.e., 10 m below the ground surface). However, regardless of the level of the groundwater table, no influence of  $n$  exists on the V/H ratio in the long periods.

#### 4.4 Influence of ground motion intensity

Figure 8 shows the V/H ratio of the different input motions. As the intensity of the input motion increases, the  $T_p$  of the vertical responses (with the groundwater table less than 10 m) remains similar (approximately 0.9 s) but that of the horizontal motion shifts toward the long periods (0.8 s to 1.5 s). As a result, the  $T_p$  of the V/H ratio remains similar as the predominant period of vertical response dominates it, as shown in Figure 8. However, as the intensity increases, the V/H ratio generally increases for all the periods especially at the  $T_p$  because the strong shaking induces more damping in the horizontal direction than the vertical direction due to more nonlinearity generated for a large strain in the horizontal direction (Figure 5). As a result, the V/H ratio is magnified.

## 5 CONCLUSIONS

In this study, the factors that could influence the V/H ratio are evaluated on the basis of the vertical and horizontal site response analyses. Vertical site response analysis is performed by following the procedure by Tsai and Liu (2017). Different intensities of vertical and horizontal motions fixed with a constant V/H ratio (i.e., 2/3) are propagated through generic sites with various groundwater tables (0, 5, and 10 m, and dry), soil porosities (approximate  $n=0.26$  to 1.12), and the corresponding wave velocity profiles. The V/H ratio at the ground surface is then calculated and compared with that at the bedrock.

The results show that the V/H ratio at the ground surface exceeds 2/3 for the period ranges between 0.1 and 1.0 s. The shape of the V/H ratio spectrum is dominated by that of the vertical spectrum. Therefore, the peak value of the V/H ratio occurs during short periods (approximately 0.1 s) associated with the site periods of  $V_p$ . A site with the lowest groundwater table (i.e., dry condition) and the highest porosity tends to amplify the V/H ratio. In addition, the V/H ratio increases with the intensity of the input motion due to different behaviors of vertical and horizontal wave propagation.



## ACKNOWLEDGEMENT

The authors gratefully acknowledge the support given by the Ministry of Science and Technology in Taiwan under Award No. MOST 105-2628-E-005-002- MY3.

## REFERENCES

- Ambraseys, N. N. & Douglas, J. (2003) Near-field horizontal and vertical earthquake ground motions. *Soil Dynamics and Earthquake Engineering*, 23(1), 1-18.
- Bozorgina, Y., Niazi, M. & Campbell, K. W. (1995) Characteristics of free-field vertical ground motion during the Northridge earthquake. *Earthquake Spectra*, 11, 515-525.
- G Lerce, Z. & Abrahamson, N. A. (2010) Vector-valued probabilistic seismic hazard assessment for the effects of vertical ground motions on the seismic response of highway bridges. *Earthquake Spectra* 26, 26, 999-1016.
- G Lerce, Z. & Abrahamson, N. A. (2011) Site-specific design spectra for vertical ground motion. *Earthquake Spectra*, 27, 1023-1047.
- Hardin, B. O. & Drnevich, V. P. (1972) Shear modulus and damping in soils: Measurement and parameter effects. *Journal of Soil Mechanics and Foundation Engineering Division*, 98, 603-624.
- Hashash, Y.M.A., Musgrove, M.I., Harmon, J.A., Groholski, D.R., Phillips, C.A., and Park, D. (2016). DEEPSOIL 6.1, User Manual. Urbana, IL, Board of Trustees of University of Illinois at Urbana-Champaign.
- Kunnath, S. K., Erduran, E., Chai, Y. H. & Yashinsky, M. (2008) Effect of near-fault vertical ground motions on seismic response of highway overcrossings. *Journal of Bridge Engineering*, ASCE, 13, 282-290.
- Liu, H. W. & Tsai, C. C. (2018) site effect of vertical motion ? amplification behavior observed from downhole arrays. *Journal of GeoEngineering*, 13, 39-48.
- Masing, G. (1926) *Eigenspannungen und Verfestigung beim Messing*. Second International Congress on Applied Mechanics. Zurich, Switzerland.
- NCEER (1997) FHWA/NCEER workshop on national representation of seismic ground motion for new and existing highway facilities. Technical report, NCEER-97-0010.
- Newmark, N. M. & Hall, W. J. (1978) Seismic Design Criteria for Pipelines and Facilities. *Journal of the Technical Councils of ASCE*, 104, 91-107.
- Seed, H. B. & Idriss, I. M. (1970) Soil moduli and damping factors for dynamic response analyses, Berkeley, College of Engineering University of California Berkeley.
- Stewart, J. P., Boore, D. M., Seyhan, E. & Atkinson, G. M. (2016) NGA-West2 Equations for Predicting Vertical-Component PGA, PGV, and 5%-Damped PSA from Shallow Crustal Earthquakes. *Earthquake Spectra*, 32, 1005-1031.
- Tsai, C. C. & Liu, H. W. (2017) Site response analysis of vertical ground motion in consideration of soil nonlinearity. *Soil Dynamics and Earthquake Engineering*, 102, 124-136.
- Wang, Z. (2008) Damage and lessons of the great Wenchuan earthquake.
- Yang, J. & Lee, C. M. (2007) Characteristics of vertical and horizontal ground motions recorded during the Niigata-ken Chuetsu, Japan Earthquake of 23 October 2004. *Engineering Geology*, 94(1-2), 50-64.
- Yang, J. & Sato, T. (2000) Interpretation of seismic vertical amplification observed at an array site. *Bulletin of the Seismological Society of America*, 90, 275-285.
- Yang, J. & Yan, X. R. (2009) Factors affecting site response to multi-directional earthquake loading. *Engineering Geology*, 107, 77-87.